universe

MDPI

Article

Anisotropic Compact Stars in General Relativity: An Exact Self-Bound Analytical Solution for Stellar Systems

Sunil Kumar Maurya [1,2,*], Ghulam Mustafa [3], Faisal Javed [3], Saibal Ray [4], Assmaa Abd-Elmonem [5] and Neissrien Alhubieshi [5]

[1] Department of Mathematical and Physical Sciences, College of Arts and Sciences, University of Nizwa, P.O. Box 33, Nizwa 616, Oman
[2] Research Center of Astrophysics and Cosmology, Khazar University, 41 Mehseti Street, Baku AZ1096, Azerbaijan
[3] Department of Physics, Zhejiang Normal University, Jinhua 321004, China; gmustafa3828@gmail.com (G.M.); faisaljaved.math@gmail.com (F.J.)
[4] Centre for Cosmology, Astrophysics and Space Science (CCASS), GLA University, Mathura 281406, Uttar Pradesh, India; saibal.ray@gla.ac.in
[5] Department of Mathematics, College of Science, King Khalid University, Abha 61421, Saudi Arabia; aahaasn@kku.edu.sa (A.A.-E.); nalhbshi@kku.edu.sa (N.A.)
* Correspondence: sunil@unizwa.edu.om

Abstract: In the present work, we investigate anisotropic compact stars under the general relativistic platform. Following a novel technique, we found an exact self-bound analytical stellar solution. The obtained solution was matched on the spherical surface of the boundary to the Schwarzschild metric in order to find the expressions of the constants involved in the neutral system. We conducted various critical investigations such as on the variations in pressures, density, energy conditions, pressure–density ratios, the velocity of sounds, and gravitational potentials within stellar objects. We also conducted a stability analysis of the models using the cracking concepts and the adiabatic index. The values of the constant parameters were taken corresponding to the secondary components of GW190814 to validate the physical viability of our solution. This study provides fruitful results that are physically viable and, hence, satisfactory.

Keywords: general relativity; compact star; anisotropic system; exact solution

Received: 19 November 2024
Revised: 30 December 2024
Accepted: 3 January 2025
Published: 21 January 2025

Citation: Maurya, S.K.; Mustafa, G.; Javed, F.; Ray, S.; Abd-Elmonem, A.; Alhubieshi, N. Anisotropic Compact Stars in General Relativity: An Exact Self-Bound Analytical Solution for Stellar Systems. *Universe* **2025**, *11*, 33. https://doi.org/10.3390/universe11020033

1. Introduction

The breakthrough paper of 1915 by Einstein [1] introduces general relativity (GR) but does not prove a unique description about space and time with a geometry based on a metric-tensor. According to GR, the spacetime is nothing but a four-dimensional fabric which is under the control of a set of specific field equations and, thus, can explain physical activities. As J.A. Wheeler states in the dramatic fashion, "spacetime tells matter how to move; matter tells spacetime how to curve" [2]. Thus, the Newtonian "force" takes place in GR as a "field" which facilitates the understanding pf astrophysical [3] and cosmological [4] phenomena, as was initially attempted by Schwarzschild in 1916 and Einstein in 1917. This gravitational theory remained successful in the sense that at the large scale (i.e., in the non-quantum realm), all the experimental tests (e.g., geodetic deviation, frame dragging, gravitational lensing, gravitational redshift, gravity waves, and black holes) have passed smoothly.

Under the framework of GR, normal stars may come to their endpoint and, thus, form white dwarfs, neutron stars, and black holes, which are collectively known as compact stars.

They have a few common features, such as (i) a high density, though black holes have an exceptional structure, (ii) strong gravity, (iii) endpoints of stellar evolution, and (iv) stellar remnants that are generally non-radiating in the classical sense [5]. However, nowadays, the source of fast radio bursts (FRBs), i.e., compact object mergers and magnetars, are also being included in the above-mentioned group [6,7]. In the context of the formation scenario, an active star may eventually take shape either into a compact star (when the inward gravitational attraction is greater than the outward radiative pressure) or a supernova (when the outward radiative pressure is greater than the inward gravitational attraction). However, in the theoretical context, a few hypothetical compact stars, e.g., quark stars, Boson stars, etc., may be formed via phase transition and some other processes. There is interesting research that suggests that compact stars could also form during the phase separations of the early universe following the Big Bang [8].

To avoid mathematical complexity, a compact star in astrophysics is normally assumed to be filled with isotropic fluid, which means that the radial component of the pressure ($P_r(r)$) is the same as that with the angular component ($P_t(r)$). However, this assumption represents a highly specialized case; rather, an anisotropic property is a general feature of the internal fluid so that the pressure components become unequal, which means that $P_r(r) \neq P_t(r) (\equiv P_\theta(r) = P_\phi(r))$. This situation gives rise to anisotropy at each interior point of the fluid configuration, which can be attributed to the non-zero spatial gradient of the scalar field. As a result, the hydrostatic Tolman–Oppenheimer–Volkoff (TOV) equation for an anisotropic stellar configuration has been discussed in the works of Tolman and Oppenheimer–Volkoff [9,10]. The anisotropy factor, represented by the symbol Δ, is the quantitative measure of the difference between P_t and P_r, i.e., $\Delta = P_t - P_r$. Regarding anisotropic stars in the GR framework, Mak and Harko [11] discussed a lot at a basic level of astrophysical platform. In connection to this work [11], one may also note the following from the exact solutions that"All the solutions we have obtained are non-singular inside the anisotropic sphere, with finite values of the density and pressure at the center of the star". Interested readers are requested to consult a few more exact solutions that are available in the literature [12–14]. However, long ago, the effect of anisotropy on a relativistic stellar system was studied by Ruderman [15] based on the argument that in the high density (i.e., $\rho > 10^{15}$ gm/cm^3), the relativistic interaction occurs within nuclear matter, and this process produces anisotropy as an inherent property of the system. Later on, several other scientists also investigated this issue of anisotropy [16–19].

The above-mentioned studies have revealed that the sources giving rise to pressure anisotropy in any self-gravitating stellar system may mainly be of the following kinds: (i) the existence of superfluidity in the core, (ii) phase transitions, (iii) the presence of a magnetic field, (iv) rotational motion, (v) the presence of mix fluids, (vi) tidal effects, and several other reasons. According to Bowers and Liang [16], in the presence of complex strong interactions, both superfluidity and superconductivity provide causal effect for anisotropy. On the other hand, the origin of local anisotropy in stellar systems was extensively reviewed in Ref. [17]. In another work, Herrera showed that even if a stellar system is initially considered with an isotropic matter distribution, due to the internal physical processes within the system, it always tends to produce pressure anisotropy [20]. Some other interesting works in the context of pressure anisotropy are available in the following works: [11,21–37].

The scheme of the present work is as follows: In Section 2, we provide Einstein's general relativistic field equations for compact stars. In Section 3, a novel analytical solution for the anisotropic spherical model is presented for a stellar system. In Section 4, we discuss the necessary junction conditions at the boundary of the object to find the constants involved in the solution. We conduct several critical tests to understand the

physical features of the stellar object, as discussed in Section 5. Lastly, in Section 6, we present relevant discussion and comments regarding the results of the present investigation.

2. General Relativistic Field Equations for the Stellar Configuration

The Einstein field equations can be formulated in the following manner:

$$\mathcal{R}^i_j - \frac{1}{2}\mathcal{R}\, g^i{}_j = -\kappa T^i_j, \tag{1}$$

where $\kappa = 8\pi$ and $c = G = 1$.

we consider a static and spherically symmetric spacetime that defines the internal structure of the object as

$$ds^2 = F_0^2(r)\, dt^2 - H_0^2(r) dr^2 - r^2(d\theta^2 + \sin^2\theta\, d\phi^2). \tag{2}$$

The functions $F_0(r)$ and $H_0(r)$ are gravitational potentials solely determined by the radial coordinate r. The stellar object is believed to contain an anisotropic matter distribution. As a result, T^i_j represents the energy-momentum tensor of the fluid distribution given by

$$T^i_j = (\rho + P_t)u^i u_j - P_t\, \delta^i{}_j + (P_r - P_t)\mathcal{N}^i\mathcal{N}_j. \tag{3}$$

In the above, the formula for u^i is $F_0 u^i = \delta^i_4$, where u^i denotes the four-velocity. The symbol $\mathcal{N}^i$ denotes a unit vector in the direction of the radial motion, expressed as $H_0\mathcal{N}^i = \delta^i{}_1$, whereas ρ denotes the energy density. The form of P_r is referred to as the radial pressure and the variable P_t denotes the pressure that is perpendicular to $\mathcal{N}_i$, often referred to as the transverse or tangential pressure. In addition, T^1_1 is equivalent to $-P_r$. The values of T^2_2 and T^3_3 are both equivalent to $-P_t$. The expression $T^4_4 = \rho$ denotes the fourth element of the matter distribution.

Within the context of the spherically symmetric metric (2), the Einstein field equations may be written as the system of ordinary differential equations:

$$\frac{1}{r^2}\left[\frac{F_0 + 2F_0' r}{F_0 H_0^2} - 1\right] = \kappa P_r, \tag{4}$$

$$\frac{-H_0'(F_0 + F_0' r) + H_0(F_0' + F_0'' r)}{F_0 H_0^3 r} = \kappa P_t, \tag{5}$$

$$\frac{H_0^3 - H_0 + 2H_0' r}{H_0^3 r^2} = \kappa \rho, \tag{6}$$

where the prime symbol denotes differentiation with respect to r.

The metric expression might be utilized to determine the mass function of a fluid sphere, denoted as $m(r)$ and $\mathcal{H}_0(r)$, given by

$$\frac{1}{H_0^2} = 1 - \frac{2m(r)}{r}. \tag{7}$$

Equations (6) and (7) allow us to describe their mass $m(r)$ with respect to the energy density

$$m(r) = \frac{\kappa}{2}\int \rho\, r^2 dr, \tag{8}$$

which essentially follows from the definition of the Misner–Sharp mass function [38] in the case of spherically symmetric physical configuration.

By using Equations (4) and (7), we may derive the following:

$$\frac{2F'}{F_0}\left(1-\frac{2m}{r}\right)=\kappa\, r P_r+\frac{2m}{r^2}. \tag{9}$$

The gradient of pressure can be quantified by employing Equations (4)–(7) which include mass, energy density, and pressures along with Equation (9) as follows:

$$\frac{dP_r}{dr}=-\left(\kappa r P_r+\frac{2m}{r^2}\right)\left(1-\frac{2m}{r}\right)^{-1}(P_r+\rho)+\frac{2\Delta}{r}, \tag{10}$$

where Equation (10) denotes a hydrostatic TOV equation for an anisotropic stellar configuration.

3. A Novel Analytical Solution for the Anisotropic Spherical Model

In this section, we focus on finding a new exact anisotropic solution to the field Equations (4)–(6) for the compact star model. Therefore, we use the pressure anisotropy condition obtained by subtracting the Equations (4) and (5) as follows:

$$\Delta=\frac{1}{8\pi F_0 H_0^3 r^2}\left[r(H_0F_0''r-H_0F_0'-F_0'H_0'r)-F\left(H_0-H_0^3+H_0'r\right)\right]. \tag{11}$$

Now, the master Equation (11) contains three unknowns: F_0, H_0, and Δ. Therefore, to solve this master Equation (11), we consider the ansatz for the metric $H_0(r)$ corresponding to Buchdahl solution [39], as follows:

$$H_0^2=\frac{\mathrm{Y}_1(1+\mathrm{Y}_2r^2)}{\mathrm{Y}_1+\mathrm{Y}_2r^2}, \tag{12}$$

where Y_1 and Y_2 are two factors that define the geometry of the objects.

The fact that the interior Schwarzschild solution may be recovered for $\mathrm{Y}_1=0$ and that the hypersurfaces $\{t=\text{constant}\}$ become flat for $\mathrm{Y}_1=1$ is a fascinating characteristic of the Buchdahl solution. Additionally, it is to be noted that assumption $\mathrm{Y}_2=-\mathrm{Y}_1/R^2$ allows one to recover the Vaidya and Tikekar [40] solution, whereas for $\mathrm{Y}_1=-2$, one can obtain the Durgapal and Bannerji [41] solution. The most general exact isotropic solution was investigated by Gupta–Jasim [42], where they showed that the solution for $0<\mathrm{Y}_1<1$ does not exhibit a negative gradient of energy density, i.e., the density is either increasing in nature or non-positive within the stellar model. As a consequence, we must neglect this region.

By substituting Equation (10) into Equation (12), we obtain

$$\frac{F_0''}{F_0}-\frac{F_0'\left(r^4\mathrm{Y}_2^2+\mathrm{Y}_1\left(2r^2\mathrm{Y}_2+1\right)\right)}{F_0r(r^2\mathrm{Y}_2+1)(r^2\mathrm{Y}_2+\mathrm{Y}_1)}-\frac{\Delta\mathrm{Y}_1\left(r^2\mathrm{Y}_2+1\right)}{(r^2\mathrm{Y}_2+\mathrm{Y}_1)}=\frac{r^2(1-\mathrm{Y}_1)\mathrm{Y}_2^2}{(r^2\mathrm{Y}_2+1)(r^2\mathrm{Y}_2+\mathrm{Y}_1)}. \tag{13}$$

For the stable celestial configurations, anisotropy should vanish at the core, meaning that pressures P_r and P_t are equal at the center. Furthermore, the anisotropic force $\frac{2(P_t-P_r)}{r}$ generated by anisotropy must be positive, i.e., it should be repulsive.

Under such constraints, we consider the anisotropy

$$\Delta=\frac{r^2(\mathrm{Y}_1-1)\mathrm{Y}_2^2}{\mathrm{Y}_1(r^2\mathrm{Y}_2+1)^2}. \tag{14}$$

The above expression for Δ vanishes at $r = 0$, while it is positive throughout the stellar object. After plugging this expression of Δ into Equation (14), we find the final form of the master equation:

$$\frac{F_0''}{F_0} - \frac{F_0'\left(r^4\mathrm{Y}_2^2 + \mathrm{Y}_1\left(2r^2\mathrm{Y}_2 + 1\right)\right)}{F_0 r(r^2\mathrm{Y}_2 + 1)(r^2\mathrm{Y}_2 + \mathrm{Y}_1)} = 0. \tag{15}$$

Now, we compute the final form of the metric function F_0 after integrating the above Equation (15) as follows:

$$F_0 = \frac{1}{2\sqrt{r^2\mathrm{Y}_2 + \mathrm{Y}_1}}\left[C_0\left(\frac{r^2\left(r^2\mathrm{Y}_2 + \mathrm{Y}_1\right)}{\sqrt{r^2\mathrm{Y}_2 + 1}} + \frac{r^2\mathrm{Y}_2 + \mathrm{Y}_1}{\mathrm{Y}_2\sqrt{r^2\mathrm{Y}_2 + 1}}\right.\right.$$
$$\left.\left. - \frac{\sqrt{\mathrm{Y}_2}(\mathrm{Y}_1 - 1)^3\sqrt{\frac{r^2\mathrm{Y}_2 + \mathrm{Y}_1}{\mathrm{Y}_1 - 1}}\sinh^{-1}\left(\frac{\sqrt{\mathrm{Y}_2}\sqrt{r^2\mathrm{Y}_2 + 1}}{\sqrt{(\mathrm{Y}_1 - 1)\mathrm{Y}_2}}\right)}{((\mathrm{Y}_1 - 1)\mathrm{Y}_2)^{3/2}}\right)\right] + D_0, \tag{16}$$

where C_0 and D_0 are integration constants.

We are now in a position to determine the precise expression for the pressures and density as follows:

$$8\pi\rho = \frac{(\mathrm{Y}_1 - 1)\mathrm{Y}_2\left(r^2\mathrm{Y}_2 + 3\right)}{\mathrm{Y}_1(r^2\mathrm{Y}_2 + 1)^2}, \tag{17}$$

$$8\pi P_r = \left[4C_0\mathrm{Y}_2^{5/2}\left(r^2\mathrm{Y}_2 + \mathrm{Y}_1\right)\right]\left[\mathrm{Y}_1\left(C_0 r^4\mathrm{Y}_2^{7/2} + C_0 r^2\mathrm{Y}_2^{5/2} + C_0 r^2\mathrm{Y}_1\mathrm{Y}_2^{5/2} - C_0((\mathrm{Y}_1 - 1)\mathrm{Y}_2)^{3/2}\sqrt{r^2\mathrm{Y}_2 + 1}\right.\right.$$
$$\left.\left.\times\sqrt{\frac{r^2\mathrm{Y}_2 + \mathrm{Y}_1}{\mathrm{Y}_1 - 1}}\sinh^{-1}\left(\frac{\sqrt{\mathrm{Y}_2}\sqrt{r^2\mathrm{Y}_2 + 1}}{\sqrt{(\mathrm{Y}_1 - 1)\mathrm{Y}_2}}\right) + C_0\mathrm{Y}_1\mathrm{Y}_2^{3/2} + 2D_0\mathrm{Y}_2^{5/2}\sqrt{r^2\mathrm{Y}_2 + 1}\sqrt{r^2\mathrm{Y}_2 + \mathrm{Y}_1}\right)\right]^{-1}$$
$$- \frac{(\mathrm{Y}_1 - 1)\mathrm{Y}_2}{\mathrm{Y}_1(r^2\mathrm{Y}_2 + 1)}, \tag{18}$$

$$8\pi P_t = \left[4C_0\mathrm{Y}_2^{5/2}\left(r^2\mathrm{Y}_2 + \mathrm{Y}_1\right)\right]\left[\mathrm{Y}_1\left(C_0 r^4\mathrm{Y}_2^{7/2} + C_0 r^2\mathrm{Y}_2^{5/2} + C_0 r^2\mathrm{Y}_1\mathrm{Y}_2^{5/2} - C_0((\mathrm{Y}_1 - 1)\mathrm{Y}_2)^{3/2}\sqrt{r^2\mathrm{Y}_2 + 1}\right.\right.$$
$$\left.\left.\times\sqrt{\frac{r^2\mathrm{Y}_2 + \mathrm{Y}_1}{\mathrm{Y}_1 - 1}}\sinh^{-1}\left(\frac{\sqrt{\mathrm{Y}_2}\sqrt{r^2\mathrm{Y}_2 + 1}}{\sqrt{(\mathrm{Y}_1 - 1)\mathrm{Y}_2}}\right) + C_0\mathrm{Y}_1\mathrm{Y}_2^{3/2} + 2D_0\mathrm{Y}_2^{5/2}\sqrt{r^2\mathrm{Y}_2 + 1}\sqrt{r^2\mathrm{Y}_2 + \mathrm{Y}_1}\right)\right]^{-1}$$
$$+ \frac{(\mathrm{Y}_1 - 1)\mathrm{Y}_2}{\mathrm{Y}_1(r^2\mathrm{Y}_2 + 1)} + \frac{r^2(\mathrm{Y}_1 - 1)\mathrm{Y}_2^2}{\mathrm{Y}_1(r^2\mathrm{Y}_2 + 1)^2}. \tag{19}$$

4. Junction Conditions at the Boundary of the Object

For simplicity, we assume that the star is motionless and does not emit any radiation, and the outer part of the star is expected to be free of normal matter. Hence, the outside region of spacetime is characterized by the Schwarzschild metric:

$$ds^2 = \left(1 - \frac{2M}{r}\right)dt^2 - r^2(d\theta^2 + \sin^2\theta d\phi^2) - \left(1 - \frac{2M}{r}\right)^{-1}dr^2, \tag{20}$$

where r is greater than $2M$, with M being the entire mass of the stellar object.

Under this situation, the relevant criteria that need to be taken into account are

$$(g_{rr})^{-}_{interior} = (g_{rr})^{+}_{exterior}, \tag{21}$$
$$(g_{tt})^{-}_{interior} = (g_{tt})^{+}_{exterior}. \tag{22}$$
$$P_r(R) = 0. \tag{23}$$

The continuity of the metric potential across the surface, $r = R$, provides

$$F_0^2(R) = 1 - \frac{2M}{R}, \tag{24}$$
$$H_0^2(R) = \left(1 - \frac{2M}{R}\right)^{-1}. \tag{25}$$

Therefore, the junction conditions (24), (25), and (23) create a facility to calculate the following expressions for the constants:

$$\mathrm{Y}_1 = \frac{R^3\mathrm{Y}_2}{R^2\mathrm{Y}_2(R-2M)-2M}, \tag{26}$$

$$D_0 = \left[\sqrt{1-\frac{2M}{R}}\left(R^4\mathrm{Y}_2^{5/2}\left(10M^2-9MR+2R^2\right)+2M^2\sqrt{R^2\mathrm{Y}_2+1}\sqrt{-\frac{R^2\mathrm{Y}_2(2M-R)}{M}}\right.\right.$$
$$\times\sqrt{-\frac{M\mathrm{Y}_2(R^2\mathrm{Y}_2+1)}{R^2\mathrm{Y}_2(2M-R)+2M}}\sinh^{-1}\left(\frac{\sqrt{\mathrm{Y}_2}\sqrt{R^2\mathrm{Y}_2+1}}{\sqrt{\mathrm{Y}_2\left(\frac{R^3\mathrm{Y}_2}{R^2\mathrm{Y}_2(R-2M)-2M}-1\right)}}\right)+5MR^2\mathrm{Y}_2^{3/2}$$
$$\left.\left.\times(2M-R)\right)\right]\Bigg/\left[2R^2\mathrm{Y}_2^{3/2}\left(R^2\mathrm{Y}_2(R-2M)-2M\right)(R-2M)\right], \tag{27}$$

$$C_0 = D_0\left[2M\mathrm{Y}_2^{3/2}\sqrt{\frac{R^2\mathrm{Y}_2(2M-R)(R^2\mathrm{Y}_2+1)}{R^2\mathrm{Y}_2(2M-R)+2M}}\left(R^2\mathrm{Y}_2(R-2M)-2M\right)\right]\Bigg/\left[\sqrt{R^2\mathrm{Y}_2+1}\right.$$
$$\times\left(R^4\mathrm{Y}_2^{5/2}\left(10M^2-9MR+2R^2\right)+2M^2\sqrt{R^2\mathrm{Y}_2+1}\sqrt{-\frac{R^2\mathrm{Y}_2(2M-R)}{M}}\sqrt{-\frac{M\mathrm{Y}_2(R^2\mathrm{Y}_2+1)}{R^2\mathrm{Y}_2(2M-R)+2M}}\right.$$
$$\times\sinh^{-1}\left(\frac{\sqrt{\mathrm{Y}_2}\sqrt{R^2\mathrm{Y}_2+1}}{\sqrt{\mathrm{Y}_2\left(\frac{R^3\mathrm{Y}_2}{R^2\mathrm{Y}_2(R-2M)-2M}-1\right)}}\right)$$
$$\left.\left.+5MR^2\mathrm{Y}_2^{3/2}(2M-R)\right)\right]. \tag{28}$$

5. Critical Investigations on Physical Characteristics of the Stellar Object

In this section, we would like to critically investigate a few physical characteristics of our model on the stellar object, which are as follows:

1. **Regularity of the gravitational potentials:** In order to remain a well-behaved solution, it is necessary for the derived gravitational potentials for the model to be finite at the core of the object. Here, the potential $H_0^2(0) = 1$, while the central value of $F_0^2(r)$ is

given by

$$F_0^2(0) = \left[\left(\frac{Y_1}{Y_2} - \frac{\sqrt{\frac{Y_1}{Y_1-1}}\sqrt{Y_2}}{((Y_1-1)Y_2)^{3/2}}\sinh^{-1}\left(\frac{\sqrt{Y_2}}{\sqrt{(Y_1-1)Y_2}}\right)\right) \times\frac{C_0(Y_1-1)^3}{2\sqrt{Y_1}} + D_0\right]^2 = \text{constant and non-singular.} \quad (29)$$

Furthermore, it can be easily verified that $F_0'(0) = 0$ and $F_0''(0) > 0$. Equations (12) and (16), along with Equation (29), clearly indicate that the gravitational potentials within the star are finite as well as positive. These statements suggest that the metric is smooth at the center and has excellent characteristics across the celestial body, as evident from Figure 1. We note from Figure 1 that the metric potential $F_0^2(r)$ is roughly steady and keeps its behavior as it is along the radial coordinate r, whereas the $H_0^2(r)$ is gradually increasing with r, which is inversely related to $F_0^2(r)$. Now, one may look at Figure 2, where the expected features are available as the mentioned two gravitational potentials are inversely proportional. However, those do not exactly match on the boundary; rather, they meet at the radius $R \sim 10.8$ km of the star under consideration, and this radius, therefore, provides us the physical configuration of the star, i.e., the radius of the compact star. From the figure, it is clear that the intrinsic metric remains well behaved, i.e., free from the central singularity, smoothly connected and without any discontinuity at the stellar boundary $r > R$. It is also notable that below $R \sim 10.8$ km, where $r = 2M$, a coordinate singularity occurs and, thus, one obtains there the Schwarzschild sphere with the radius $R_S = 7.88$ km. Beyond the region, where $R \sim 10.8$ km, we obtain an unusual and extra feature due to the ergospheric effect, with an indication that the pressures do not vanish on the boundary of the compact star (see Figure 2, upper right panel).

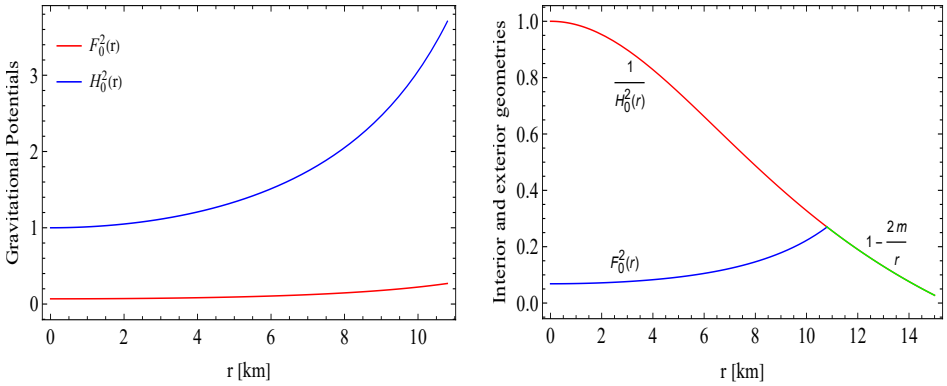

Figure 1. The gravitational potentials $F_0^2(r)$ and $H_0^2(r)$ (**left panel**), and (**right panel**) interior and exterior geometries along the radial distance r for the values of the physical parameters and constants $R = 10.8$ km, $M = 2.67\ M_\odot$, $Y_1 = -1.95$, $Y_2 = 0.008$ km^{-2}, and $R_{sch} = 7.88$ km.

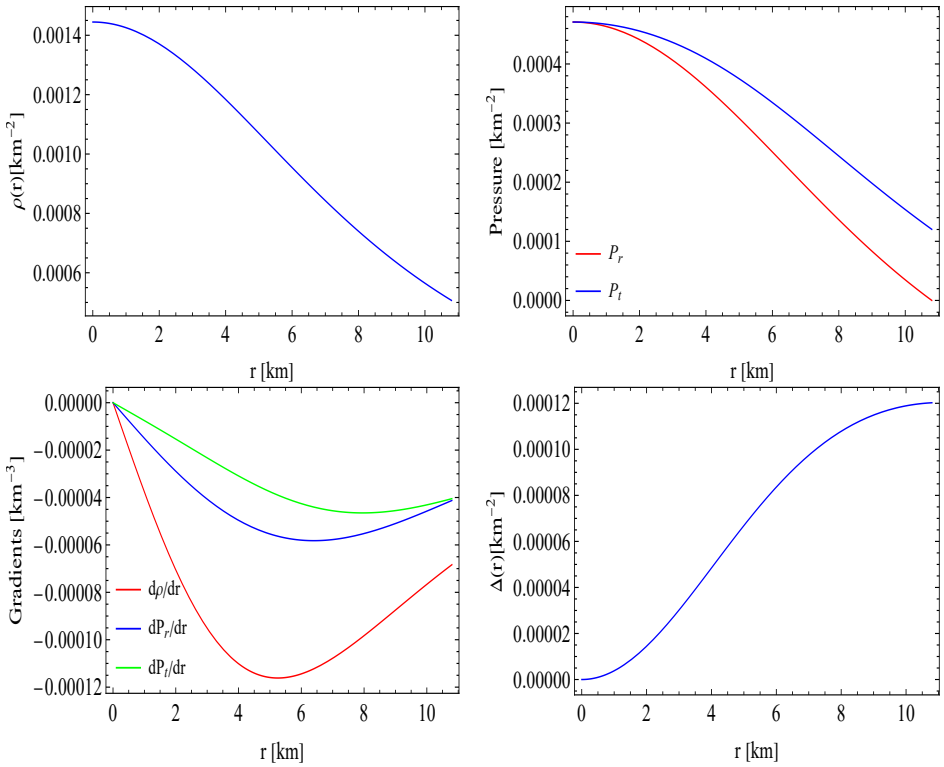

Figure 2. (i) Energy density $\rho(r)$ (**upper left** panel) and (ii) the radial and tangential pressures P_r and P_t (**upper right** panel), (iii) density and pressures gradients ($\frac{d\rho}{dr}$, $\frac{dP_r}{dr}$, and $\frac{dP_t}{dr}$) (**lower left** panel), and (ii) anisotropy (Δ) (**lower right** panel) along the radial distance r for the values of the physical parameters and constants $R = 10.8$ km, $M = 2.67\ M_{\odot}$, $\mathrm{Y}_1 = -1.95$, $\mathrm{Y}_2 = 0.008$ km^{-2}, and $R_{sch} = 7.88$ km.

2. **Pressure and Density Profiles at the Core of the Star:**
For a realistic model of a compact star, it is essential for the physical quantities ρ, P_r, and P_t to have positive values and consistently decline, i.e., $d\rho/dr$, dP_r/dr, and dP_t/dr must be negative for $r > 0$. In our given situation, to verify these criteria, we first calculate the gradients of these variables by using the following specific procedure:

$$8\pi\frac{d\rho}{dr} = -\frac{2r(\mathrm{Y}_1-1)\mathrm{Y}_2^2(r^2\mathrm{Y}_2+5)}{\mathrm{Y}_1(r^2\mathrm{Y}_2+1)^3}, \tag{30}$$

$$8\pi\frac{dP_r}{dr} = \frac{8C_0 r\mathrm{Y}_2^{7/2}}{\Psi_1(r)} - \frac{\Psi_2(r)}{\Psi_3(r)} + \frac{2r(\mathrm{Y}_1-1)\mathrm{Y}_2^2}{\mathrm{Y}_1(r^2\mathrm{Y}_2+1)^2}, \tag{31}$$

$$8\pi\frac{dP_t}{dr} = \frac{r\mathrm{Y}_2^2}{\Psi_4^2(r)\mathrm{Y}_1(r^2\mathrm{Y}_2+1)^3}\Big[4\Psi_4(r)\Psi_6(r)+\Psi_7(r) \times\Psi_6(r)\Big(r^2\mathrm{Y}_2+1\Big) - \Psi_4(r)\Psi_5(r)\Big(r^2\mathrm{Y}_2+1\Big)\Big], \tag{32}$$

where the explicit expressions for all the components used in the above equations are given in Appendix A.

Moreover, there must be a finite and non-negative value for the central density and central radial as well as tangential pressures inside the system. In the current model, the central values of these quantities are

$$\rho(0) = \frac{3(\mathrm{Y}_1 - 1)\mathrm{Y}_2}{8\pi \mathrm{Y}_1}, \tag{33}$$

$$P_r(0) = P_t(0) = \left[4C_0\mathrm{Y}_2^{5/2}\left(r^2\mathrm{Y}_2 + \mathrm{Y}_1\right)\right] \Big/ \left[\mathrm{Y}_1\left(C_0 r^4 \mathrm{Y}_2^{7/2} + C_0 r^2 \mathrm{Y}_2^{5/2} + C_0 r^2 \mathrm{Y}_1 \mathrm{Y}_2^{5/2}\right.\right.$$
$$-C_0((\mathrm{Y}_1 - 1)\mathrm{Y}_2)^{3/2}\sqrt{r^2\mathrm{Y}_2 + 1}\sqrt{\frac{r^2\mathrm{Y}_2 + \mathrm{Y}_1}{\mathrm{Y}_1 - 1}}\sinh^{-1}\left(\frac{\sqrt{\mathrm{Y}_2}\sqrt{r^2\mathrm{Y}_2 + 1}}{\sqrt{(\mathrm{Y}_1 - 1)\mathrm{Y}_2}}\right)$$
$$\left.\left.+C_0\mathrm{Y}_1\mathrm{Y}_2^{3/2} + 2D_0\mathrm{Y}_2^{5/2}\sqrt{r^2\mathrm{Y}_2 + 1}\sqrt{r^2\mathrm{Y}_2 + \mathrm{Y}_1}\right)\right]^{-1} - \frac{(\mathrm{Y}_1 - 1)\mathrm{Y}_2}{\mathrm{Y}_1(r^2\mathrm{Y}_2 + 1)}. \tag{34}$$

To ensure the feature of the positive density and pressure at the center, the parameters Y_2 must be positive, while Y_1 must be either $\mathrm{Y}_1 > 1$ or $\mathrm{Y}_1 < 0$, i.e., $\mathrm{Y}_1 \notin [0,1]$. Therefore, the positivity of Equation (34) gives

$$\frac{D_0}{C_0} < \frac{-\mathrm{Y}_1\mathrm{Y}_2^{3/2} + \frac{4\mathrm{Y}_2^{3/2}}{1-\frac{1}{\mathrm{Y}_1}} + \sqrt{\frac{\mathrm{Y}_1}{\mathrm{Y}_1-1}}((\mathrm{Y}_1 - 1)\mathrm{Y}_2)^{3/2}\sinh^{-1}\left(\frac{\sqrt{\mathrm{Y}_2}}{\sqrt{(\mathrm{Y}_1-1)\mathrm{Y}_2}}\right)}{2\sqrt{\mathrm{Y}_1}\mathrm{Y}_2^{5/2}}. \tag{35}$$

Since the pressure–density ratio must be less than unity everywhere within the star, i.e., $\frac{P_r(0)}{\rho(0)} = \frac{P_t(0)}{\rho(0)} < 1$, we have

$$\frac{D_0}{C_0} > \frac{4\left(4 - \frac{4}{\mathrm{Y}_1}\right)\mathrm{Y}_2^{3/2} - \mathrm{Y}_1\mathrm{Y}_2^{3/2} + \sqrt{\frac{\mathrm{Y}_1}{\mathrm{Y}_1-1}}((\mathrm{Y}_1 - 1)\mathrm{Y}_2)^{3/2}\sinh^{-1}\left(\frac{\sqrt{\mathrm{Y}_2}}{\sqrt{(\mathrm{Y}_1-1)\mathrm{Y}_2}}\right)}{2\sqrt{\mathrm{Y}_1}\mathrm{Y}_2^{5/2}}. \tag{36}$$

Using the inequalities (35) and (36), we obtain

$$\frac{4\left(4 - \frac{4}{\mathrm{Y}_1}\right)\mathrm{Y}_2^{3/2} - \mathrm{Y}_1\mathrm{Y}_2^{3/2} + \sqrt{\frac{\mathrm{Y}_1}{\mathrm{Y}_1-1}}((\mathrm{Y}_1 - 1)\mathrm{Y}_2)^{3/2}\sinh^{-1}\left(\frac{\sqrt{\mathrm{Y}_2}}{\sqrt{(\mathrm{Y}_1-1)\mathrm{Y}_2}}\right)}{2\sqrt{\mathrm{Y}_1}\mathrm{Y}_2^{5/2}} < \frac{D_0}{C_0}$$
$$< \frac{-\mathrm{Y}_1\mathrm{Y}_2^{3/2} + \frac{4\mathrm{Y}_2^{3/2}}{1-\frac{1}{\mathrm{Y}_1}} + \sqrt{\frac{\mathrm{Y}_1}{\mathrm{Y}_1-1}}((\mathrm{Y}_1 - 1)\mathrm{Y}_2)^{3/2}\sinh^{-1}\left(\frac{\sqrt{\mathrm{Y}_2}}{\sqrt{(\mathrm{Y}_1-1)\mathrm{Y}_2}}\right)}{2\sqrt{\mathrm{Y}_1}\mathrm{Y}_2^{5/2}}. \tag{37}$$

Furthermore, the $P_r(0) = P_t(0)$ condition indicates that the anisotropy disappears at the center. Overall, the behaviors of the pressure and density profiles are satisfactory under our stellar model, as can be observed from Figure 2.

Now, we will establish the relation between the parameters R, Y_1, and Y_2 through the following condition:

$$\frac{d\Delta}{dr} = -\frac{2r(\mathrm{Y}_1 - 1)\mathrm{Y}_2^2(r^2\mathrm{Y}_2 - 1)}{\mathrm{Y}_1(r^2\mathrm{Y}_2 + 1)^3} = 0. \tag{38}$$

After solving Equation (38) we obtain the following relation:

$$r = \sqrt{\frac{1}{\mathrm{Y}_2}}. \tag{39}$$

From Equation (39) and Figure 3, it is clear how the parameter Y_2 affects the radius of the star. However, it is observed that Y_1 has no impact on r, but if Y_2 decreases, then the value of r increases.

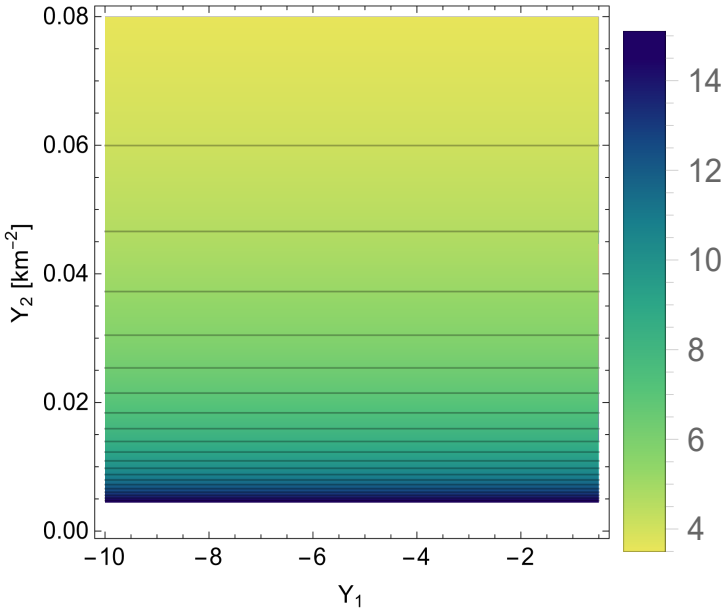

Figure 3. Density plot of r over the parameters Y_1 and Y_2.

3. **Equation of state parameter:** The equation of state (EOS) parameter is defined as the quotient of the pressure divided by the density, which provides important information on the composition of the star's substance and the characteristics of maximum mass for a compact star [43]. Furthermore, the parameter P_i/ρ must not exceed 1 throughout the entire stellar configuration. Therefore, we consider to examine our model via the equation of state parameters, defined by

$$\omega_r = \frac{P_r}{\rho}, \quad \omega_t = \frac{P_t}{\rho}. \tag{40}$$

In order to obtain a non-exotic ω_i where $i = \{r, t\}$, its value must fall between 0 and 1, and one can note that the criteria are shown to be satisfied by our model, i.e., $0 \leq \omega_r \leq 1$ and $0 \leq \omega_t \leq 1$, taking place in the first quadrant of the graphical plot (see Figure 4). In this context, it will be worthwhile to mention that $\omega = 1$ represents a case of stiff fluid, as envisioned by Zel'dovich [44], where the pressure P is equal to the energy density ρ, which means that the speed of sound in the fluid is equal to the speed of light. On the other hand, $\omega = 1/3$ is the EOS parameter for photons, and to achieve this phase we need $\rho = 3P$ such that ω needs to exceed $2/3$ from the stiff fluid EOS parameter. We draw a line to highlight the situation for $w = 1/3$ in Figure 3.

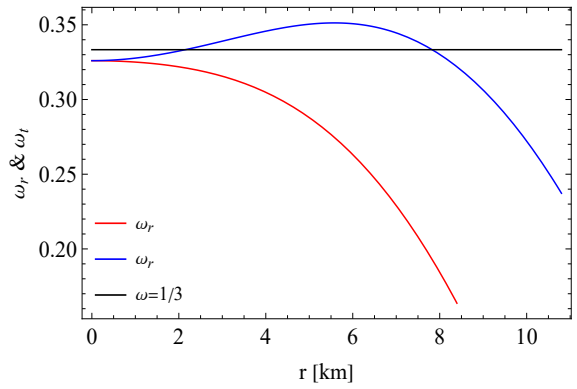

Figure 4. Equation of state parameter ω_r and ω_t along the radial distance r for the values of the physical parameters and constants $R = 10.8$ km, $M = 2.67\ M_\odot$, $Y_1 = -1.95$, $Y_2 = 0.008$ km^{-2}, and $R_{sch} = 7.88$ km.

4. **Causality condition:** The radial and transverse speed of sound ($c = 1$) can be obtained as follows:

$$v_r^2 = \frac{dP_r}{d\rho} \text{ and } v_t^2 = \frac{dP_t}{d\rho}, \tag{41}$$

where the expressions for v_r^2 and v_r^2 can be directly determined from Equations (30)–(32). In order to make a relativistic anisotropic star physically acceptable, the quantities v_r^2 and v_t^2 inside the star must be less than 1. This means that the rate of change of P_r and P_t with respect to ρ ($dP_r/d\rho$ and $dP_r/d\rho$) must be between 0 and 1. This condition is referred to as the causality condition, which is depicted in Figure 5. It can be noted from this figure that the sound speeds are increasing with the radial distance, while a contrary feature is exhibited by the stability factor.

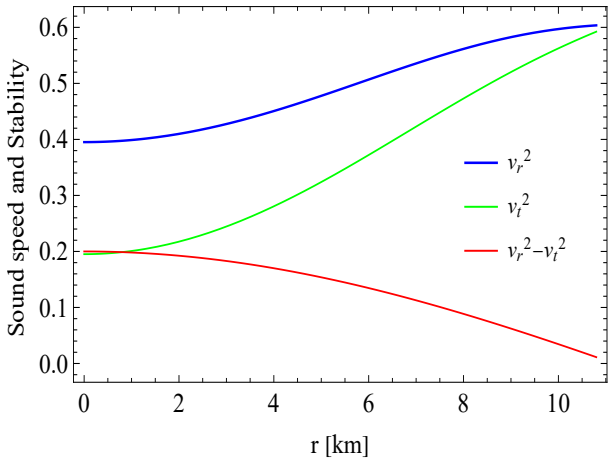

Figure 5. Radial and transverse speed of sounds (v_r^2 & v_t^2) as well as stability factor ($v_r^2 - v_t^2$) along the radial distance r for the values of the physical parameters and constants $R = 10.8$ km, $M = 2.67\ M_\odot$, $Y_1 = -1.95$, $Y_2 = 0.008$ km^{-2}, and $R_{sch} = 7.88$ km.

5. **Energy conditions:** The classical energy requirements are useful for forecasting the characteristics of the matter within the dense star. In general, the energy conditions may be summarized as follows:

(i) Null energy condition (NEC): $\rho + P_i \geq 0$.
(ii) Weak energy condition (WEC): $\rho + P_i \geq 0$, $\rho \geq 0$.
(iii) Strong energy condition (SEC): $\rho + P_i \geq 0$, $\rho + \sum P_i \geq 0$.
(iv) Dominant energy condition (DEC): $\rho - P_i \geq 0$.
(v) Trace energy condition (TEC): $\rho - P_r - 2P_t \geq 0$.

It should be noted that the energy conditions are satisfied by all normal or Newtonian matter. To examine the status of the linear barotropic equation, we write

$$\sum P_i = \omega\rho, \tag{42}$$

where the strong energy condition necessitates $\omega \geq -1$. Figure 6 shows that our model is satisfying all the energy conditions; therefore, it provides regular matter that may represent the quadratic equation of state.

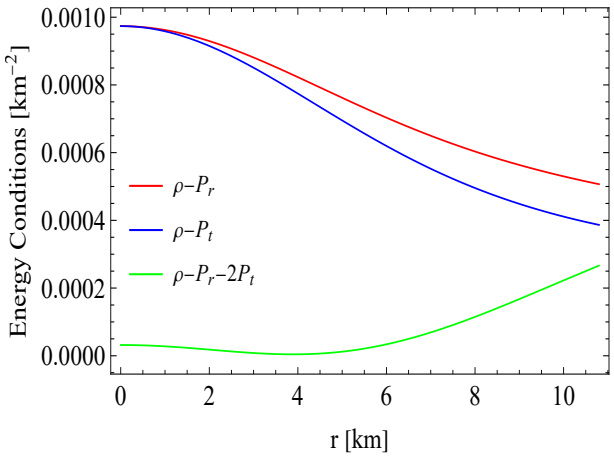

Figure 6. Energy conditions along the radial distance r for the values of the physical parameters and constants $R = 10.8$ km, $M = 2.67\ M_{\odot}$, $\mathrm{Y}_1 = -1.95$, $\mathrm{Y}_2 = 0.008$ km^{-2}, and $R_{sch} = 7.88$ km.

6. **Stability via Harrison–Zel'dovich–Novikov (HZN) criteria:** When determining stability, we make use of the criteria of Harrison–Zel'dovich–Novikov (HZN) [45,46]. For the purpose of determining the scientific reliability of the HZN stability criterion, the following inequality is utilized:
   - $\frac{dM}{d\rho_0} > 0 \quad \rightarrow$ Stable stellar structure.
   - $\frac{dM}{d\rho_0} < 0 \quad \rightarrow$ Unstable stellar structure.

   Here, ρ_0 denotes a central density.
   In order to verify the above condition for an anisotropic solution, we determine the subsequent expressions:

$$M = \frac{4\pi\rho_0 r^3(\mathrm{Y}_1 - 1)}{\mathrm{Y}_1(8\pi\rho_0 r^2 + 3) - 3}, \tag{43}$$

$$\frac{dM}{d\rho_0} = \frac{12\pi r^3(\mathrm{Y}_1 - 1)^2}{(\mathrm{Y}_1(8\pi\rho_0 r^2 + 3) - 3)^2}. \tag{44}$$

From Figure 7, one can observe that $\frac{dM}{d\rho_0} > 0$ and, thus, provides a stable stellar structure.

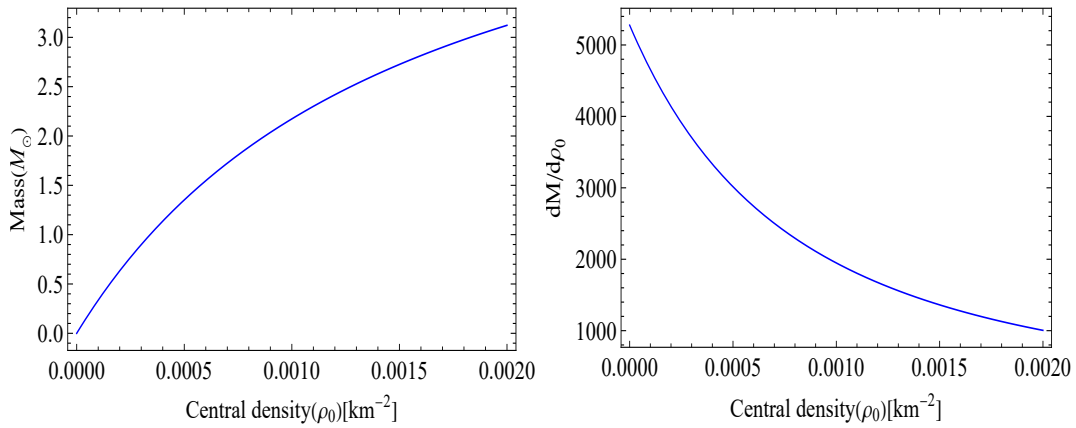

Figure 7. (i) Mass ($M/M_{\odot}$) in the (**left**) panel and (ii) mass gradient ($dM/d\rho_0$) in the (**right**) panel along the central density ρ_0 for the values of the physical parameters and constants $R = 10.8$ km, $M = 2.67\ M_{\odot}$, $\mathrm{Y}_1 = -1.95$, $\mathrm{Y}_2 = 0.008$ km^{-2}, and $R_{sch} = 7.88$ km.

7. **Stability via adiabatic index:** The definition of the adiabatic index

$$\Gamma_r = \frac{P_r + \rho}{P_r}\left(\frac{dP_r}{d\rho}\right), \tag{45}$$

is a factor that determines the stability of a relativistic anisotropic star structure. According to the notion of Heintzmann and Hillebrandt [47], a Newtonian isotropic sphere is considered to be in stable equilibrium if the adiabatic index Γ_r becomes greater than $4/3$, whereas if it is equal to $4/3$, the isotropic sphere will be in neutral equilibrium. However, according to the recent research by Chan et al. [48], the stability of a relativistic anisotropic sphere may be determined by the following condition:

$$\Gamma_r > \frac{4}{3} - \left[\frac{4(P_r - P_t)}{3r|P_r'|}\right]_{max}. \tag{46}$$

Figure 8 features the stability under the adiabatic index, which starts from a numerical value that is greater than $4/3 = 1.33$ and increases gradually with respect to the radial coordinate.

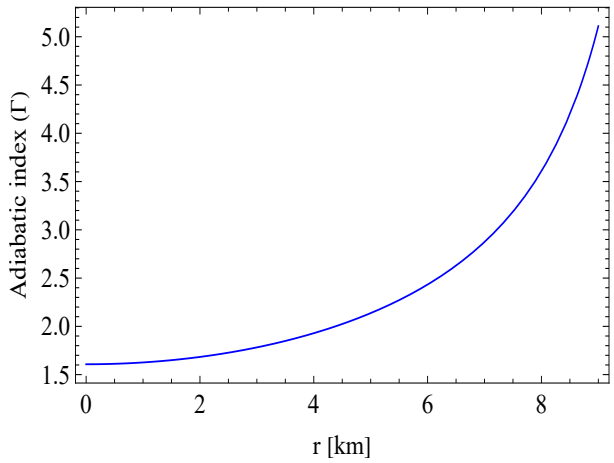

Figure 8. Adiabatic index (Γ) along the radial distance r for the values of the physical parameters and constants $R = 10.8$ km, $M = 2.67\ M_\odot$, $\Upsilon_1 = -1.95$, and $R_{sch} = 7.88$ km.

8. **Hydrostatic equilibrium via TOV criterion:** A stellar object remains in a state of static equilibrium due to the forces acting on it, specifically the gravitational force (F_g), hydrostatic force (F_h), and anisotropic force (F_a). The mathematical formulation of this condition is known as the Tolman–Oppenheimer–Volkoff (TOV) equation and can be given by

$$-\frac{dP_r}{dr} - \frac{F_0'}{F_0}(P_r + \rho) + \frac{2(P_t - P_r)}{r} = 0. \tag{47}$$

The above equation can be divided into three mentioned forces, viz., F_g, F_h, and F_a, such that

$$F_g + F_h + F_a = 0, \tag{48}$$

where $F_h = -\frac{dP_r}{dr}$, $F_g = -\frac{F_0'}{F_0}(P_r + \rho)$, and $F_a = \frac{2(P_t - P_r)}{r}$.

We note from Figure 9 that the gravitational force is much higher than the combined forces of the hydrostatic and anisotropy. However, the stability is maintained in the stellar system due to mutual balancing between the forces.

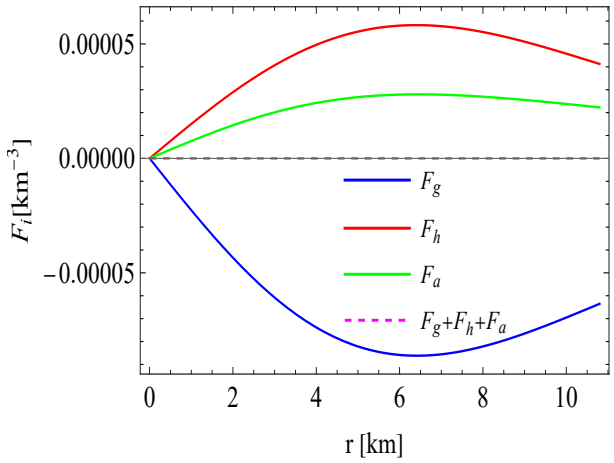

Figure 9. Different forces F_g, F_h, and F_a along the radial distance r for the values of the physical parameters and constants $R = 10.8$ km, $M = 2.67\ M_\odot$, $\mathrm{Y}_1 = -1.95$, $\mathrm{Y}_2 = 0.008$ km^{-2}, and $R_{sch} = 7.88$ km.

6. Discussion and Conclusions

In the presented research article, our aim was to investigate anisotropic compact stars in the framework of general relativity. We employed a novel technique to obtain an exact self-bound analytical solution to the stellar configuration. As usual, we matched inner solutions to the external Schwarzschild metric on the bounding surface to obtain relationships for the constants.

It is interesting to note that the physical characteristics of our stellar model are satisfactory as far as the nature of the plots are concerned. Let us, therefore, have some salient features of the presented model, via the graphical plots, which can be exhibited as follows:

(i) In order to obtain an idea regarding the nature of the proposed solution and whether it remains well behaved, we draw Figure 1 for the derived gravitational potentials for the model to be finite at the core of the object. It can be noted that the functions $F_0(r)$ and $H_0^2(r)$ are unconstrained and solely determined by the radial coordinate r. Figure 1 clearly indicates that the gravitational potentials within the star are both finite and positive, which readily suggests that the metric is smooth at the center and has excellent characteristics across the celestial body.

(ii) For a stellar model to be physically acceptable, there must be a finite and non-negative value for the central density, central radial, and tangential pressure inside the configuration. For the current stellar model, all the central values of these quantities are satisfactory, as evident from Figure 2. Moreover, Figure 3 shows the variation of radial distance r over the parameters Y_1 and Y_2.

(iii) The equation of state parameter provides important information regarding the composition of the internal stellar substance and the characteristics of maximum mass for a compact star, as can be observed from Figure 4.

(iv) The features of the radial and transverse speed of sound can be obtained from Figure 5, which essentially ensures the causality condition. In order to make a relativistic anisotropic star physically acceptable, the quantities v_r^2 and v_t^2 inside the star must be less than 1. This can be understood in the following way: the rate of change of P_r and P_t with respect to ρ ($dP_r/d\rho$ and $dP_r/d\rho$) must remain in between 0 and 1. Thus, from this figure, one can observe that the condition has been maintained appreciably.

(v) As the classical energy conditions are useful in the context of forecasting the attributes of the matter within the dense stellar configuration, we exhibit the energy budgeting in Figure 6. This figure shows the usual features as per physical requirements.

(vi) The stability of the stellar configuration via the HZN criteria is demonstrated in Figure 7

(vii) Stability via the adiabatic index is shown in Figure 8, and determines the stability of a relativistic anisotropic star structure in a satisfactory manner.

(viii) Furthermore, the hydrostatic equilibrium via the Tolman–Oppenheimer–Volkoff (TOV) criterion, where a stellar object remains in a state of static equilibrium due to the forces acting on it, can be visualized in Figure 9.

Based on the above graphically visual scenario (i.e., Figures 1–9), we would like to conclude that the current study represents a physically consistent and interesting anisotropic model of stellar systems under the framework of general relativity. In this context, one may look into Tables 1 and 2 for comparative studies for the presented model and other exact solutions, as available in the literature [14,33,49–51].

Table 1. Values of physical parameters of the secondary component of GW190814 (2.67 $M_{\odot}$) with radius $R = 10.8$ km, $Y_1 = -1.95$, $Y_2 = 0.008\,\mathrm{km}^{-2}$ where $P_{i0} = P_r(r=0) = P_t(r=0)$, $\rho_0 = \rho(r=0)$, $\rho_s = \rho(r=R)$, $P_{ts} = P_t(r=R)$.

Central Pressure P_{i0} (dyne/cm^2)	Surface Pressure P_{ts} (dyne/cm^2)	Central Density ρ_0 (gm/cm^3)	Surface Density ρ_s (gm/cm^3)
5.72149×10^{35}	1.46084×10^{35}	1.94972×10^{15}	6.84024×10^{14}

Table 2. Values of physical parameters of the secondary component of GW190814 (2.67 $M_{\odot}$) with radius $R = 10.8$ km, $Y_1 = -1.95$, $Y_2 = 0.008\,\mathrm{km}^{-2}$ where $P_{i0} = P_r(r=0) = P_t(r=0)$, $\rho_0 = \rho(r=0)$, $\rho_s = \rho(r=R)$, $P_{ts} = P_t(r=R)$.

$M-R$ Ratio (M/R)	Adiabatic Index (Γ)	Surface Redshift (Z)
0.36512	1.60737	0.92536

Author Contributions: Conceptualization, S.K.M., G.M., F.J., S.R., A.A.-E. and N.A.; Methodology, S.K.M., G.M. and S.R.; Software, S.K.M. and G.M.; Validation, S.K.M., G.M., F.J., S.R., A.A.-E. and N.A.; formal analysis, S.K.M., G.M., F.J., S.R., A.A.-E. and N.A.; data curation, S.K.M., G.M. and S.R.; writing—original draft preparation, S.K.M., G.M., F.J., S.R., A.A.-E. and N.A.; writing—review and editing, S.K.M., G.M., F.J., S.R., A.A.-E. and N.A.; project administration: S.K.M., G.M. and S.R. All authors have read and agreed to the published version of the manuscript.

Funding: The authors extend their appreciation to the Deanship of Research and Graduate Studies at King Khalid University for funding this work through Large Research Project under grant number RGP2/334/45.

Data Availability Statement: No new data has been generated.

Acknowledgments: The authors extend their appreciation to the Deanship of Research and Graduate Studies at King Khalid University for funding this work through Large Research Project under grant number RGP2/334/45. The author SKM is thankful for continuous support and encouragement from the administration of University of Nizwa. S.R. is thankful to the authority of Inter-University Centre for Astronomy and Astrophysics, Pune, India, for providing the Visiting Associateship under which a part of this work was carried out.

Conflicts of Interest: The authors declare no conflicts of interest.

Appendix A

$$\Psi_1(r) = \mathrm{Y}_1\Bigg(C_0 r^4 \mathrm{Y}_2^{7/2} + C_0 r^2 \mathrm{Y}_2^{5/2} + C_0 r^2 \mathrm{Y}_1 \mathrm{Y}_2^{5/2} - C_0((\mathrm{Y}_1-1)\mathrm{Y}_2)^{3/2}\sqrt{r^2\mathrm{Y}_2+1}\sqrt{\frac{r^2\mathrm{Y}_2+\mathrm{Y}_1}{\mathrm{Y}_1-1}}$$
$$\times \sinh^{-1}\left(\frac{\sqrt{\mathrm{Y}_2}\sqrt{r^2\mathrm{Y}_2+1}}{\sqrt{(\mathrm{Y}_1-1)\mathrm{Y}_2}}\right) + C_0\mathrm{Y}_1\mathrm{Y}_2^{3/2} + 2D_0\mathrm{Y}_2^{5/2}\sqrt{r^2\mathrm{Y}_2+1}\sqrt{r^2\mathrm{Y}_2+\mathrm{Y}_1}\Bigg),$$

$$\Psi_2(r) = 4C_0 r \mathrm{Y}_2^{7/2}\left(r^2\mathrm{Y}_2+\mathrm{Y}_1\right)\Bigg(-\frac{C_0\sqrt{(\mathrm{Y}_1-1)\mathrm{Y}_2}\mathrm{Y}_2\left(2r^2\mathrm{Y}_2+\mathrm{Y}_1+1\right)\sinh^{-1}\left(\frac{\sqrt{\mathrm{Y}_2}\sqrt{r^2\mathrm{Y}_2+1}}{\sqrt{(\mathrm{Y}_1-1)\mathrm{Y}_2}}\right)}{\sqrt{r^2\mathrm{Y}_2+1}\sqrt{\frac{r^2\mathrm{Y}_2+\mathrm{Y}_1}{\mathrm{Y}_1-1}}}$$
$$+C_0(\mathrm{Y}_1+3)\mathrm{Y}_2^{3/2} + \mathrm{Y}_2^{5/2}\left(4C_0r^2 + \frac{2D_0\left(2r^2\mathrm{Y}_2+\mathrm{Y}_1+1\right)}{\sqrt{r^2\mathrm{Y}_2+1}\sqrt{r^2\mathrm{Y}_2+\mathrm{Y}_1}}\right)\Bigg),$$

$$\Psi_3(r) = \mathrm{Y}_1\Bigg(C_0 r^4 \mathrm{Y}_2^{7/2} + C_0 r^2 \mathrm{Y}_2^{5/2} + C_0 r^2 \mathrm{Y}_1 \mathrm{Y}_2^{5/2} - C_0((\mathrm{Y}_1-1)\mathrm{Y}_2)^{3/2}\sqrt{r^2\mathrm{Y}_2+1}\sqrt{\frac{r^2\mathrm{Y}_2+\mathrm{Y}_1}{\mathrm{Y}_1-1}}$$
$$\times \sinh^{-1}\left(\frac{\sqrt{\mathrm{Y}_2}\sqrt{r^2\mathrm{Y}_2+1}}{\sqrt{(\mathrm{Y}_1-1)\mathrm{Y}_2}}\right) + C_0\mathrm{Y}_1\mathrm{Y}_2^{3/2} + 2D_0\mathrm{Y}_2^{5/2}\sqrt{r^2\mathrm{Y}_2+1}\sqrt{r^2\mathrm{Y}_2+\mathrm{Y}_1}\Bigg)^2,$$

$$\Psi_4(r) = \sqrt{(\mathrm{Y}_1-1)\mathrm{Y}_2}\mathrm{Y}_2\left(C_0 r^2\mathrm{Y}_1 + C_0 r^2 + 2D_0\sqrt{r^2\mathrm{Y}_2+1}\sqrt{r^2\mathrm{Y}_2+\mathrm{Y}_1}\right) + C_0 r^4\sqrt{(\mathrm{Y}_1-1)\mathrm{Y}_2}\mathrm{Y}_2^2$$
$$-C_0(\mathrm{Y}_1-1)qrt\mathrm{Y}_2\sqrt{r^2\mathrm{Y}_2+1}\sqrt{\frac{r^2\mathrm{Y}_2+\mathrm{Y}_1}{\mathrm{Y}_1-1}}\sinh^{-1}\left(\frac{\sqrt{\mathrm{Y}_2}\sqrt{r^2\mathrm{Y}_2+1}}{\sqrt{(\mathrm{Y}_1-1)\mathrm{Y}_2}}\right) + C_0\sqrt{(\mathrm{Y}_1-1)\mathrm{Y}_2}\mathrm{Y}_1,$$

$$\Psi_5(r) = \frac{2\sqrt{(\mathrm{Y}_1-1)\mathrm{Y}_2}\left(C_0\left(\mathrm{Y}_1^2-8\mathrm{Y}_1-5\right)\sqrt{r^2\mathrm{Y}_2+1}\sqrt{r^2\mathrm{Y}_2+\mathrm{Y}_1} + 2D_0 r^2(\mathrm{Y}_1-1)\mathrm{Y}_2^2 + D_0\left(\mathrm{Y}_1^2-1\right)\mathrm{Y}_2\right)}{\sqrt{r^2\mathrm{Y}_2+1}\sqrt{r^2\mathrm{Y}_2+\mathrm{Y}_1}}$$
$$-24C_0 r^4\mathrm{Y}_2^2\sqrt{(\mathrm{Y}_1-1)\mathrm{Y}_2} - 12C_0 r^2(\mathrm{Y}_1+3)\mathrm{Y}_2\sqrt{(\mathrm{Y}_1-1)\mathrm{Y}_2}$$
$$-\frac{C_0(\mathrm{Y}_1-1)^2\sqrt{\mathrm{Y}_2}\sqrt{r^2\mathrm{Y}_2+1}\sinh^{-1}\left(\frac{\sqrt{\mathrm{Y}_2}\sqrt{r^2\mathrm{Y}_2+1}}{\sqrt{(\mathrm{Y}_1-1)\mathrm{Y}_2}}\right)}{\sqrt{\frac{r^2\mathrm{Y}_2+\mathrm{Y}_1}{\mathrm{Y}_1-1}}} - \frac{C_0(\mathrm{Y}_1-1)^3\sqrt{\mathrm{Y}_2}\sqrt{\frac{r^2\mathrm{Y}_2+\mathrm{Y}_1}{\mathrm{Y}_1-1}}\sinh^{-1}\left(\frac{\sqrt{\mathrm{Y}_2}\sqrt{r^2\mathrm{Y}_2+1}}{\sqrt{(\mathrm{Y}_1-1)\mathrm{Y}_2}}\right)}{\sqrt{r^2\mathrm{Y}_2+1}}$$
$$-C_0\sqrt{(\mathrm{Y}_1-1)\mathrm{Y}_2}(\mathrm{Y}_1-1)^2,$$

$$\Psi_6(r) = \sqrt{(\mathrm{Y}_1-1)\mathrm{Y}_2}\mathrm{Y}_2\Big(\mathrm{Y}_1\left(2D_0\sqrt{r^2\mathrm{Y}_2+1}\sqrt{r^2\mathrm{Y}_2+\mathrm{Y}_1} - 8C_0r^2\right) + C_0 r^2\mathrm{Y}_1^2 - 5C_0r^2 - 2D_0\sqrt{r^2\mathrm{Y}_2+1}$$
$$\times\sqrt{r^2\mathrm{Y}_2+\mathrm{Y}_1}\Big) - 4C_0 r^6\mathrm{Y}_2^3\sqrt{(\mathrm{Y}_1-1)\mathrm{Y}_2} - 3C_0 r^4(\mathrm{Y}_1+3)\mathrm{Y}_2^2\sqrt{(\mathrm{Y}_1-1)\mathrm{Y}_2} - C_0(\mathrm{Y}_1-1)^3\sqrt{\mathrm{Y}_2}$$
$$\times\sqrt{r^2\mathrm{Y}_2+1}\sqrt{\frac{r^2\mathrm{Y}_2+\mathrm{Y}_1}{\mathrm{Y}_1-1}}\sinh^{-1}\left(\frac{\sqrt{\mathrm{Y}_2}\sqrt{r^2\mathrm{Y}_2+1}}{\sqrt{(\mathrm{Y}_1-1)\mathrm{Y}_2}}\right) + C_0\sqrt{(\mathrm{Y}_1-1)\mathrm{Y}_2}(\mathrm{Y}_1-5)\mathrm{Y}_1,$$

$$\Psi_7(r) = 2\sqrt{(\mathrm{Y}_1-1)\mathrm{Y}_2}\left(C_0\mathrm{Y}_1 + C_0 + \frac{D_0\mathrm{Y}_2\left(2r^2\mathrm{Y}_2+\mathrm{Y}_1+1\right)}{\sqrt{r^2\mathrm{Y}_2+1}\sqrt{r^2\mathrm{Y}_2+\mathrm{Y}_1}}\right) + 4C_0r^2\sqrt{(\mathrm{Y}_1-1)\mathrm{Y}_2}\mathrm{Y}_2$$
$$-\frac{C_0(\mathrm{Y}_1-1)\sqrt{\mathrm{Y}_2}\sqrt{r^2\mathrm{Y}_2+1}}{\sqrt{\frac{r^2\mathrm{Y}_2+\mathrm{Y}_1}{\mathrm{Y}_1-1}}}\sinh^{-1}\left(\frac{\sqrt{\mathrm{Y}_2}\sqrt{r^2\mathrm{Y}_2+1}}{\sqrt{(\mathrm{Y}_1-1)\mathrm{Y}_2}}\right) - \frac{C_0(\mathrm{Y}_1-1)^2\sqrt{\mathrm{Y}_2}\sqrt{\frac{r^2\mathrm{Y}_2+\mathrm{Y}_1}{\mathrm{Y}_1-1}}}{\sqrt{r^2\mathrm{Y}_2+1}}$$
$$\times\sinh^{-1}\left(\frac{\sqrt{\mathrm{Y}_2}\sqrt{r^2\mathrm{Y}_2+1}}{\sqrt{(\mathrm{Y}_1-1)\mathrm{Y}_2}}\right) - C_0\sqrt{(\mathrm{Y}_1-1)\mathrm{Y}_2}(\mathrm{Y}_1-1).$$

References

1. Einstein, A. The Foundation of the General Theory of Relativity. *Ann. Phys.* **1916**, *49*, 769. [CrossRef]
2. Wheeler, J.A.; Ford, K. Geons, Black Holes, and Quantum Foam: A Life in Physics. Norton: New York, NY, USA, 1998.
3. Schwarzschild, K. On the Gravitational Field of a Mass Point according to Einstein's Theory. *Sitz. Deut. Akad. Wiss. Math. Phys.* **1916**, *23*, 189.
4. Einstein, A. Cosmological considerations on the general theory of relativity. *Sitz. Preuß. Akad. Wiss.* **1917**, *142*.
5. Tauris, T.M.; van den Heuvel, E.P.J. Formation and Evolution of Compact Stellar X-ray Sources. *arXiv* **2003**, arXiv:astro-ph/0303456.
6. Bernardini J., M.G. Gamma-ray bursts and magnetars: Observational signatures and predictions. *High Energy Astrophys.* **2015**, *7*, 64. [CrossRef]
7. Bhandari, S.; Sadler, E. M., Prochaska, J. X., Simha, S., Ryder, S. D., Marnoch, L.; Bannister, K.W.; Macquart, J.-P.; Flynn, C.; Phillips, C. The Host Galaxies and Progenitors of Fast Radio Bursts Localized with the Australian Square Kilometre Array Pathfinder. *Astrophys. J. Lett.* **2020**, *895*, L37. [CrossRef]
8. Khlopov, M.Y. Primordial black holes. *Res. Astron. Astrophys.* **2010**, *10*, 495. [CrossRef]
9. Tolman, R.C. Static Solutions of Einstein's Field Equations for Spheres of Fluid. *Phys. Rev.* **1939**, *55*, 364. [CrossRef]
10. Oppenheimer, J.R.; Volkoff, G.M. On Massive Neutron Cores. *Phys. Rev.* **1939**, *55*, 374. [CrossRef]
11. Mak, M.K.; Harko, T. Anisotropic Stars in General Relativity. *Proc. Roy. Soc. Lond. A* **2003**, *459*, 393. [CrossRef]
12. Harko, T.; Mak, M.K. Anisotropic charged fluid spheres in space–time dimensions. *J. Math. Phys.* **2000**, *41*, 4752. [CrossRef]
13. Harko, T.; Mak, M.K. Anisotropic relativistic stellar models. *Ann. Phys.* **2002**, *11*, 3. [CrossRef]
14. Bhar, P.; Errehymy, A.; Ray, S. Constraining physical parameters of DESs via the secondary component of the GW190814 event and other self-bound NS pulsars in $f(Q)$-gravity theory. *Eur. Phys. J. C* **2023**, *83*, 1151. [CrossRef]
15. Ruderman, R. Pulsars: Structure and Dynamics. *Annu. Rev. Astron. Astrophys.* **1972**, *10*, 427. [CrossRef]
16. Bowers, R.L.; Liang, E.P.T. Anisotropic Spheres in General Relativity. *Class. Astrophys. J.* **1974**, *188*, 657. [CrossRef]
17. Herrera, L.; Santos, N.O. Local anisotropy in self-gravitating systems. *Phys. Rep.* **1997**, *286*, 53. [CrossRef]
18. Mak, M.K.; Harko, T. An Exact Anisotropic Quark Star Model. *Chin. J. Astron. Astrophys.* **2002**, *2*, 248. [CrossRef]
19. Horvat, D.; Ilijic, S.; Marunovic, A. Radial pulsations and stability of anisotropic stars with a quasi-local equation of state. *Class. Quantum Gravit.* **2011**, *28*, 025009. [CrossRef]
20. Herrera, L. Stability of the isotropic pressure condition. *Phys. Rev. D* **2020**, *101*, 104024. [CrossRef]
21. Herrera, L.; Varela, V. Negative energy density and classical electron models. *Phys. Lett. A* **1994**, *189*, 11. [CrossRef]
22. Ivanov, B.V. Maximum bounds on the surface redshift of anisotropic stars. *Phys. Rev. D* **2002**, *65*, 104011. [CrossRef]
23. Schunck, F.E.; Mielke, E.W. Topical review: General relativistic boson stars. *Class. Quantum Gravit.* **2003**, *20*, 301. [CrossRef]
24. Usov, V.V. Electric fields at the quark surface of strange stars in the color-flavor locked phase. *Phys. Rev. D* **2004**, *70*, 067301. [CrossRef]
25. Herrera, L.; Ospino, J.; Prisco, A.D. All static spherically symmetric anisotropic solutions of Einstein's equations. *Phys. Rev. D* **2008**, *77*, 027502. [CrossRef]
26. Herrera, L.; Ospino, J.; Prisco, A.D.; Fuenmayor, E.; Troconis, O. Structure and evolution of self-gravitating objects and the orthogonal splitting of the Riemann tensor. *Phys. Rev. D* **2009**, *79*, 064025. [CrossRef]
27. Varela, V.; Rahaman, F.; Ray, S.; Chakraborty, K.; Kalam, M. Charged anisotropic matter with linear or nonlinear equation of state. *Phys. Rev. D* **2010**, *82*, 044052. [CrossRef]
28. Rahaman, F.; Jamil, M.; Ghosh, A.; Chakraborty, F. On generating some known black hole solutions. *Mod. Phys. Lett. A* **2010**, *25*, 835. [CrossRef]
29. Herrera, L.; Denmat, G.L.; Santos, N.O. Dynamical instability and the expansion-free condition. *Gen. Relativ. Gravit.* **2012**, *44*, 1143. [CrossRef]
30. Herrera, L.; Barreto, W. Newtonian polytropes for anisotropic matter. *Phys. Rev. D* **2013**, *87*, 087303. [CrossRef]
31. Herrera, L.; Prisco, A.D.; Barreto, W.; Ospino, J. Conformally flat polytropes for anisotropic matter. *Gen. Relativ. Gravit.* **2014**, *46*, 1827. [CrossRef]
32. Herrera, L. New definition of complexity for self-gravitating fluid distributions. *Phys. Rev. D* **2018**, *97*, 044010. [CrossRef]
33. Baskey, L.; Ray, S.; Das, S.; Majumder, S.; Das, A. Anisotropic compact stellar solution in general relativity. *Eur. Phys. J. C* **2023**, *83*, 307. [CrossRef]
34. Maurya, S.K.; Singh, K.N.; Govender, M.; Ray, S. Complexity-Free Anisotropic Solution of Buchdahl's Model and Energy Exchange Between Relativistic Fluids by Extended Gravitational Decoupling. *Fortsch. Phys. Prog. Phys.* **2023**, *71*, 2300023. [CrossRef]
35. Maurya, S.K.; Singh, K.N.; Govender, M.; Ray, S. Observational constraints on maximum mass limit and physical properties of anisotropic strange star models by gravitational decoupling in Einstein-Gauss-Bonnet gravity. *Mon. Not. R. Astron. Soc.* **2023**, *519*, 4303. [CrossRef]

36. Maurya, S.K.; Errehymy, A.; Singh, K.N.; Jasim, M.K.; Myrzakulov, K.; Umbetova, Z. Modeling self-bound binary compact object with a slow rotation effect and effect of electric field gradient on the mass-radius limit and moment of inertia. *J. High Energy Astrophys.* **2024**, *44*, 45–59. [CrossRef]
37. Bhar, P.; Rej, P.; Takisa, P.M.; Zubair, M. Relativistic compact stars in Tolman spacetime via an anisotropic approach. *Eur. Phys. J. C* **2021**, *81*, 531. [CrossRef]
38. Misner, C.W.; Sharp, D.H. Relativistic Equations for Adiabatic, Spherically Symmetric Gravitational Collapse. *Phys. Rev. B* **1964**, *136*, 571. [CrossRef]
39. Buchdahl, H.A. General Relativistic Fluid Spheres. *Phys. Rev.* **1959**, *116*, 1027. [CrossRef]
40. Vaidya, P.C.; Tikekar, R. Exact relativistic model for a superdense star. *J. Astrophys. Astron.* **1982**, *3*, 325 . [CrossRef]
41. Durgapal, M.C.; Bannerji, R. New analytical stellar model in general relativity. *Phys. Rev. D* **1983**, *27*, 328 . [CrossRef]
42. Gupta, Y.K.; Jasim, M.K. On most general exact solution for Vaidya-Tikekar isentropicsuperdense star. *Astrophys. Space Sci.* **2003**, *272*, 403 . [CrossRef]
43. Biswas, S.; Ghosh, S.; Ray, S.; Rahaman, F.; Guha, B.K. Strange stars in Krori–Barua spacetime under $f(R,T)$ gravity. *Ann. Phys.* **2019**, *401*, 1. [CrossRef]
44. Zeldovich, Y.B. The equation of state at ultrahigh densities and its relativistic limitations. *JETP* **1962**, *14*, 1143.
45. Harrison, B.K.; Thorne, K.S.; Wakano, M.; Wheeler, J.A. *Gravitational Theory and Gravitational Collapse*; University of Chicago Press: Chicago, IL, USA, 1965.
46. Zeldovich, Y.B.; Novikov, I.D. *Relativistic Astrophysics: Stars and Relativity*; University of Chicago Press: Chicago, IL, USA, 1971; Volume 1.
47. Heintzmann, H.; Hillebrandt, W. Neutron stars with an anisotropic equation of state: mass, redshift and stability. *Astron. Astrophys.* **1975**, *24*, 51.
48. Chan, R.; Herrera, L.; Santos, N.O. Dynamical instability for radiating anisotropic collapse. *Mon. Not. R. Astron. Soc.* **1993**, *265*, 533. [CrossRef]
49. Biswas, S.; Deb, D.; Ray, S.; Guha, B.K. Anisotropic charged strange stars in Krori-Barua spacetime under $f(R,T)$ gravity. *Ann. Phys.* **2021**, *426*, 168429. [CrossRef]
50. Maurya, S.K.; Chaudhary, H.; Ditta, A.; Mustafa, G.; Ray, S. Study of self-bound compact stars in $f(T)$ gravity and observational constraints on the model parameters. *Eur. Phys. J. C* **2024**, *84*, 603. [CrossRef]
51. Baskey, L.; Das, S.; Rahaman, F. Anisotropic compact stellar objects with a slow rotation effect. *Eur. Phys. J. C* **2024**, *84*, 92. [CrossRef]